Applications of Mathematics

Anita Windisch; Péter L. Simon

Global bifurcations in a dynamical model of recurrent neural networks

*Applications of Mathematics*, Vol. 68 (2023), No. 1, 35–50

Persistent URL: http://dml.cz/dmlcz/151495

# GLOBAL BIFURCATIONS IN A DYNAMICAL MODEL OF RECURRENT NEURAL NETWORKS

Anita Windisch, Péter L. Simon, Budapest

Received July 31, 2021. Published online November 18, 2022.

*Abstract.* The dynamical behaviour of a continuous time recurrent neural network model with a special weight matrix is studied. The network contains several identical excitatory neurons and a single inhibitory one. This special construction enables us to reduce the dimension of the system and then fully characterize the local and global codimension-one bifurcations. It is shown that besides saddle-node and Andronov-Hopf bifurcations, homoclinic and cycle fold bifurcations may occur. These bifurcation curves divide the plane of weight parameters into nine domains. The phase portraits belonging to these domains are also characterized.

*Keywords*: saddle-node; Hopf; homoclinic; cycle fold bifurcation; Hopfield model

*MSC 2020*: 34C23, 34C25, 34C37, 92B20

## 1. Introduction

Neural networks have attracted a significant mathematical interest recently, motivated both by machine learning applications and by brain activity models. Mathematical problems related to this field range from discrete time deep neural networks to continuous time dynamical system models in neuroscience. Modelling brain activity has led to several questions concerning differential equations, see, e.g., the review paper [3]. Our work focuses on continuous time dynamical models of

This work was supported by the project "Integrated program for training new generation of researchers in the disciplinary fields of computer science", No. EFOP-3.6.3-VEKOP-16-2017-00002. The project has been supported by the European Union and co-funded by the European Social Fund.

Péter L. Simon acknowledges support from Hungarian Scientific Research Fund, OTKA, (grant no. 115926) and from the Ministry of Innovation and Technology NRDI Office within the framework of the Artificial Intelligence National Laboratory Program.

Open Access funding enabled and organized by Eötvös Loránd University.

DOI: 10.21136/AM.2022.0158-21 

recurrent neural networks described by the Cowan-Wilson or Hopfield model that are systems of non-linear ordinary differential equations for the firing rates of the neurons, see, e.g., [7], Chapter 13, [16], Chapter 7, or [11], Section 6. Recurrent neural networks can be effectively applied as autoassociative memory that can easily store patterns and retrieve the stored data even from partial information and these are often used for image and speech recognition. The flow of the information is not obvious in these networks as the signals coming out from a neuron can get back to itself via other neurons.

Dynamical systems theory enables us to analyse nonlinear systems of differential equations including those models which are used in neuroscience and machine learning. It is often possible to classify the different behaviours of a model by studying how its solutions change as some parameters are varied. For example, we can determine the parameter values, for which the solution converges to a steady state or oscillation appears that can be crucial from the point of view of applications.

In this paper we investigate the behaviour of a deterministic firing rate model of neural networks in continuous time, often referred to as Hopfield or Cowan-Wilson model [13], taking the form

$$\dot{x} = Dx + Wy + I, \quad y_i = f(x_i), \tag{1.1}$$

where $x$ is the vector of membrane potentials and $y$ is the vector of firing rates of the neurons. The vector $I$ denotes the external input and matrix $D$ is a diagonal matrix. This network can be represented as a directed graph, where the nodes are the neurons and the edges are the connections between them. Each edge has a weight describing the strength of the connection and matrix $W$ contains these weights in system (1.1). The function $f$ is the increasing activation function [7].

Most results in the literature are about small networks and different special cases of the Hopfield model. First, Hopfield showed that the dynamical system has an energy function and proved that the solutions always converge to a steady state when the weight matrix $W$ is symmetric, i.e., $w_{ij} = w_{ji}$. First he proved it in discrete time, where the state of the neurons was set to 1 or $-1$ [12], but he extended his own results to continuous neural networks soon [13]. Beer and Ermentrout studied small networks where $f(x) = (1 + \exp(-x))^{-1}$ was applied as activation function and a bias term $\theta_i$ was introduced for each neuron [1], [6]. They gave examples for the existence of periodic solutions and determined the behaviour of the model as $I_i$ and $\theta_i$ are varied. Later, Beer chose the $\theta_i$ values as bifurcation parameters and approximated the bifurcation curves using hyperplanes. He estimated the probability that a randomly selected point in the parameter space is in a given domain [2]. Larger networks have also been studied by Fasoli et al., where an algebraic activation

function was applied [8], [9]. First they determined local and global bifurcations in a network which contains four different weights and $I_i$ and the weight of the self-connection of inhibitory neurons were chosen as bifurcation parameters. They also studied the behaviour of a fully homogeneous network with cubic topology, where the neurons are purely excitatory. Understanding the dynamic behaviour of populations of excitatory and inhibitory neurons has played a crucial role [4] for years and is in the focus of very recent studies explaining animal behaviour at the neuronal level [5].

While the previous results are mostly focused on the effect of the bias term $\theta$ and the external input $I$, in our recent work we studied the dynamics of the Hopfield model as some weights are varied [17]. We introduced a special case of the Hopfield model, where the number of neurons is arbitrary, the network is fully connected and the weight matrix $W$ has a special structure. This enables us to derive analytical results concerning the bifurcation curves. In this paper, we present the detailed investigation of the local bifurcation curves and extend this by the numerical study of the model to detect global bifurcations. We assume first that every signal coming from a given neuron has the same weight, i.e., $w_{ij} = w_j$ for all $i \neq j$, and the neurons are not connected to themselves directly, i.e., $w_{ii} = 0$ for all $i$. Then $W$ takes the form

$$W = \begin{pmatrix} 0 & w_2 & \dots & w_n \\ w_1 & 0 & \dots & w_n \\ \vdots & \vdots & \ddots & \vdots \\ w_1 & w_2 & \dots & 0 \end{pmatrix}.$$

We also suppose that the neurons do not receive any external input and we choose the matrix $D$ to be the identity matrix. We apply the sigmoid function $f(x) = (1 + \exp(a - bx))^{-1}$ as activation function. Then the $i$th equation of system (1.1) takes the form

$$\dot{x_i} = -x_i + \sum_{k=1}^{n} w_k f(x_k) - w_i f(x_i). \tag{1.2}$$

The paper is structured as follows. In Section 2 we reduce the system to two equations and then derive analytic formulas for the local bifurcation curves, i.e., the saddle-node and Andronov-Hopf bifurcation curves. Then in Section 3 we determine numerically the saddle homoclinic, saddle-node homoclinic and cycle fold bifurcation curves. These five bifurcation curves divide the parameter plane into nine regions. The phase portraits belonging to these parameter regions are determined in Section 4. The results are summarized and further research directions are presented in the concluding section.

## 2. Local bifurcations

The starting point of our investigation is the case when all the weights are equal and positive. This has already been studied and it turned out that with equal positive weights, system (1.2) can be reduced to a lower dimensional system [17]. More precisely, the result is the following.

**Theorem 2.1.** *If $i$ and $j$ are indices satisfying $w_i = w_j > 0$, then the function $t \mapsto |x_i(t) - x_j(t)|$ is strictly decreasing and $\lim_{t\to\infty} |x_i(t) - x_j(t)| = 0$, i.e., $x_i$ equals to $x_j$ in steady states and along periodic orbits.*

We assume below that $n-1$ neurons have the same positive weight denoted by $w$ and only one of them has a different weight denoted by $w_1$, which can be negative as well. System (1.2) can be reduced using Theorem 2.1 since $n-1$ variables tend to a common value, i.e., their asymptotic behaviour can be given by a single variable. This can be formulated as follows.

**Corollary 2.2.** *If there exists $w > 0$ such that $w = w_i$ for all $i = 2, \dots, n$ and $w_1$ is arbitrary, then it is enough to investigate the solutions of the system below to describe the asymptotic behaviour of system* (1.2),

$$\dot{x}_1 = -x_1 + (n-1)wf(x_2), \tag{2.1}$$

$$\dot{x}_2 = -x_2 + w_1 f(x_1) + (n-2)wf(x_2). \tag{2.2}$$

The local bifurcations of this system can be investigated analytically. In order to determine the saddle-node bifurcation curve we apply Sotomayor's theorem [15]. First, let $x^* = (x_1^*, x_2^*)$ denote a steady state of system (2.1)–(2.2). Now we derive a single equation for the equilibrium points given by system (2.1)–(2.2) with zeros in the left-hand sides. Substituting

$$x_1^* = (n-1)wf(x_2^*) \tag{2.3}$$

from the first equation into the second, $x_2^*$ can be calculated from the single steady state equation which takes the form

$$-x_2 + w_1 f((n-1)wf(x_2)) + (n-2)wf(x_2) = 0. \tag{2.4}$$

A parameter pair $(w, w_1)$ lies on the saddle-node curve if there exists a number $x_2$ for which equation (2.4) holds and the derivative of the right-hand side is also zero, i.e.,

$$-1 + w_1 f'((n-1)wf(x_2))wf'(x_2) + (n-2)wf'(x_2) = 0, \tag{2.5}$$

which ensures that the Jacobian matrix of system (2.1)–(2.2) has a single eigenvalue $\lambda = 0$ at the bifurcation point. Equations (2.4) and (2.5) give a parametric representation of the saddle-node curve in the parameter plane $(w, w_1)$ parametrized by $x_2$. The parameter $w_1$ can be expressed from equation (2.4) as

$$w_1 = \frac{x_2 - (n-2)wf(x_2)}{f((n-1)wf(x_2))}, \tag{2.6}$$

and can be substituted into (2.5). Two transversality conditions also have to be satisfied for the occurrence of saddle-node bifurcation. First, let $F$ be the vector of the right-hand side of system (2.1)–(2.2). Let $w^*$ denote a bifurcation point when $x^* = (x_1^*, x_2^*)$ is an equilibrium of the system, where $x_2^*$ is implicitly given by equation (2.4) in terms of $w$ and $w_1$ and $x_1^*$ can be calculated from (2.3). Let $q$ and $r$ be right and left eigenvectors of eigenvalue $\lambda = 0$:

$$q = \begin{bmatrix} (n-1)wf'(x_2) \\ 1 \end{bmatrix}, \quad r = \begin{bmatrix} w_1 f'(x_2) \\ 1 \end{bmatrix}. \tag{2.7}$$

Then the first transversality condition $r^\top [D_x^2 F(x^*, w^*)(q, q)] \neq 0$ leads to

$$(n-1)^2 w_1 f'(x_2^*)(-w_1 f'(x_1^*)^2 f''(x_2^*) + f''(x_1^*) f'(x_2^*)) + (n-2)^2 f'(x_1^*)^2 f''(x_2^*) \neq 0. \tag{2.8}$$

The other transversality condition is given by

$$r^\top \partial_w F(x^*, w^*) \neq 0, \tag{2.9}$$

where

$$\partial_w F(x^*, w^*) = \begin{bmatrix} -\dfrac{\partial x_1^*}{\partial w} + (n-1)f(x_2^*) + (n-1)wf'(x_2^*)\dfrac{\partial x_2^*}{\partial w} \\ -\dfrac{\partial x_2^*}{\partial w} + w_1 f'(x_1^*)\dfrac{\partial x_1^*}{\partial w} + (n-2)f(x_2^*) + (n-2)wf'(x_2^*)\dfrac{\partial x_2^*}{\partial w} \end{bmatrix}.$$

Derivative $\partial x_2^*/\partial w$ is used here, which is calculated from equation (2.4) by implicit differentiation

$$\frac{\partial x_2^*}{\partial w} = -\frac{(n-1)w_1 f'((n-1)wf(x_2^*))f(x_2^*) + (n-2)f(x_2^*)}{-1 + (n-1)ww_1 f'((n-1)wf(x_2^*))f'(x_2^*) + (n-2)wf'(x_2^*)}.$$

Transversality conditions can be formulated similarly when the weight $w_1$ is chosen as bifurcation parameter, which imply that

$$\frac{f''(x_2^*)}{f'(x_1^*)} + (n-1)wf''(x_1^*)f'(x_2^*)\frac{1-(n-2)wf'(x_2^*)}{f'(x_1^*)} \neq 0, \tag{2.10}$$

$$r^\top \partial_{w_1} F(x^*, w_1^*) \neq 0 \tag{2.11}$$

have to be fulfilled, where

$$\partial_{w_1} F(x^*, w_1^*) = \begin{bmatrix} -\dfrac{\partial x_1^*}{\partial w_1} + (n-1)wf'(x_2^*)\dfrac{\partial x_2^*}{\partial w_1} \\ -\dfrac{\partial x_2^*}{\partial w_1} + f(x_1^*) + w_1 f'(x_1^*)\dfrac{\partial x_1^*}{\partial w_1} + (n-2)f'(x_2^*)\dfrac{\partial x_2^*}{\partial w_1} \end{bmatrix}$$

and the derivative $\partial x_2^*/\partial w_1$ is given by the implicit derivative of (2.4) with respect to $w_1$:

$$\frac{\partial x_2^*}{\partial w_1} = \frac{f((n-1)wf(x_2^*))}{-1 + (n-1)ww_1 f'((n-1)wf(x_2^*))f'(x_2^*) + (n-2)wf'(x_2^*)}.$$

All of the transversality conditions can be checked numerically. Then the following statement can be derived from these calculations.

**Theorem 2.3.** *For a given value of $x_2$ the corresponding point (or points) $(w, w_1)$ of the saddle-node curve is given as follows. If transversality conditions* (2.9)–(2.11) *are satisfied, then the first coordinate, $w$, is given implicitly by the equation*

$$-1 + \frac{x_2 - (n-2)wf(x_2)}{f((n-1)wf(x_2))} f'((n-1)wf(x_2))(n-1)wf'(x_2) + (n-2)wf'(x_2) = 0 \tag{2.12}$$

*and the second coordinate $w_1$ is given explicitly by* (2.6).

In the case of the Andronov-Hopf bifurcation curve, both coordinates can be expressed explicitly in terms of $x_2$. The first equation of this bifurcation is again the single steady state equation (2.4). The second one is that the trace of the Jacobian of system (2.1)–(2.2) is zero subject to the condition that its determinant is positive. The trace of the Jacobian can be easily expressed as

$$\operatorname{Tr} J = -2 + (n-2)wf'(x_2).$$

For this bifurcation the transversality conditions take the form $d(\operatorname{Re}\lambda(w))/w \neq 0$ and $d(\operatorname{Re}\lambda(w_1))/w_1 \neq 0$ leading to

$$\frac{1}{2}\Big((n-2)f'(x_2^*) + (n-2)wf''(x_2^*)\frac{\partial x_2^*}{\partial w}\Big) \neq 0, \tag{2.13}$$

$$\frac{1}{2}(n-2)wf''(x_2^*)\frac{\partial x_2^*}{\partial w_1} \neq 0. \tag{2.14}$$

These conditions can be checked numerically. Hence, the Andronov-Hopf bifurcation curve can be obtained as follows.

**Theorem 2.4.** *For a given value of $x_2$ the corresponding point $(w, w_1)$ of the Andronov-Hopf bifurcation curve is given as follows. If transversality conditions* (2.13)–(2.14) *are satisfied, then the first coordinate, $w$, is*

$$w = \frac{2}{(n-2)f'(x_2)} \tag{2.15}$$

*and the second coordinate $w_1$ is given again by* (2.6).

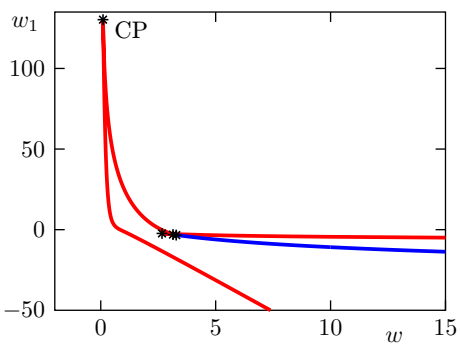


(a) A cusp point (CP) of saddle-node bifurcation curve.

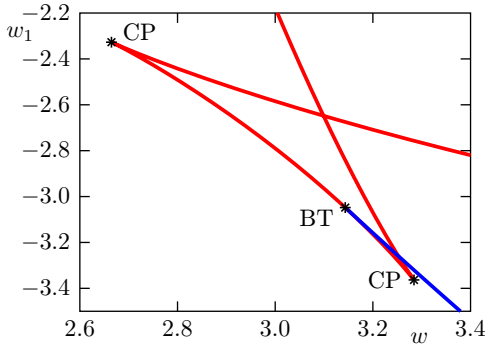


(b) The swallowtail of saddle-node-bifurcation curve with the Bogdanov-Takens (BT) bifurcation point.

Figure 1. Saddle-node (red) and Andronov-Hopf (blue) bifurcation curves in system (2.1) and (2.2) with fixed parameters $a = 4$, $b = 1$, and $n = 10$.

A typical position of the two bifurcation curves is shown in Figure 1, where we used the activation function

$$f(x) = (1 + \exp(a - bx))^{-1}$$

with fixed parameters $a = 4$, $b = 1$ and $n = 10$. In this case the saddle-node bifurcation curve (red) has a swallowtail, its cusp points are denoted by CP. The endpoint of the Andronov-Hopf bifurcation curve (blue) can be found in this swallowtail. This common point of the two bifurcation curves is the Bogdanov-Takens bifurcation point that can also be determined analytically as follows. The common point of the two bifurcation curves satisfies the equations of both, i.e., the coordinates of the Bogdanov-Takens bifurcation point satisfy equations (2.6), (2.12) and (2.15). We can plug in $w$ from (2.15) into (2.12) leading to a single equation for $x_2$. The solution of this equation yields that value of $x_2$ that belongs to the Bogdanov-Takens bifurcation point. Introducing the function

$$g(x) = \frac{2f(x)(n-1)}{f'(x)(n-2)},$$

the equation for $x_2$ takes a simpler form as it is given in the next statement.

**Theorem 2.5.** *Let $x_2^{\mathrm{BT}}$ be a solution of*

$$2\Big(\frac{n-1}{n-2}x_2 - g(x_2)\Big)f'(g(x_2)) + f(g(x_2)) = 0.$$

*Then the coordinates of a Bogdanov-Takens bifurcation point in the $(w, w_1)$ parameter plane can be given as*

$$w^{\mathrm{BT}} = \frac{2}{(n-2)f'(x_2^{\mathrm{BT}})}, \quad w_1^{\mathrm{BT}} = \frac{x_2^{\mathrm{BT}} - (n-2)w^{\mathrm{BT}}f(x_2^{\mathrm{BT}})}{f((n-1)w^{\mathrm{BT}}f(x_2^{\mathrm{BT}}))}.$$

We note that numerical experiments show that the above equation always has a single solution for $x_2$ as the parameters $a$, $b$ and $n$ are varied, i.e., there is a single Bogdanov-Takens bifurcation point.

## 3. Global bifurcation curves

Our goal here is to find the global bifurcations in the reduced two-dimensional system (2.1)–(2.2). While we could determine local bifurcations, where the phase portrait changed in a neighbourhood of a steady state, analytically, global bifurcations cannot be determined using analytical tools. In the case of global bifurcations the phase portrait changes along a global structure such as a limit cycle or a homoclinic orbit. We use the MatCont MATLAB toolbox [10], developed for the investigation of parametrized dynamical systems and also for bifurcation studies, for the detection of global bifurcations. We fix parameters of the activation function $a = 4$, $b = 1$ and the size of the network, $n = 10$, for the investigation below.

The first global bifurcation that we detect is the fold bifurcation of cycles, where two coexisting periodic orbits, a stable one and an unstable one, collide and disappear [14]. To get a cycle fold bifurcation point, a periodic orbit should be found first, for which the *ode* solvers of MATLAB are available in MatCont. Then this periodic orbit can be continued by varying one parameter until we get to the cycle fold bifurcation point denoted by LPC. The starting point of this continuation process can be the Andronov-Hopf bifurcation curve that has already been determined analytically, yielding a periodic orbit. We note that even more simply we can start from a steady state and find the Andronov-Hopf point by continuation [10]. For system (2.1)–(2.2), we used the stable limit cycle born on the Andronov-Hopf bifurcation curve, and continued it by varying the value of $w_1$ (with $w$ fixed at 900) until the limit point of cycles (LPC) is reached as it can be seen in Figure 2 (a). Once LPC is found, we can continue the unstable periodic orbit, with which the stable one collided. This way we can get information about the appearance of the unstable periodic orbit. The continuation algorithm of MatCont enables us to continue the

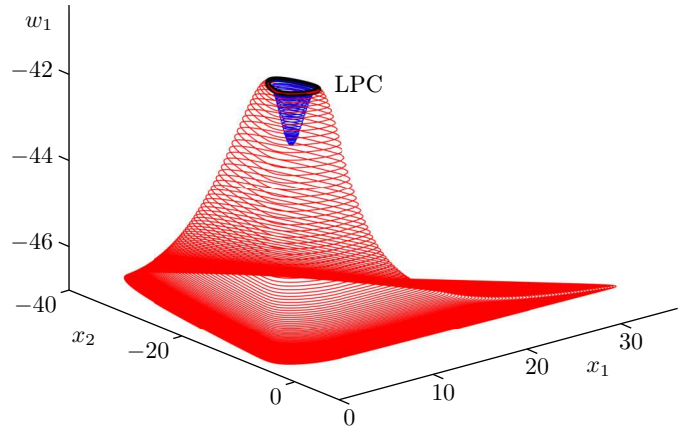


(a) Continuation of stable (blue) and unstable (red) periodic orbits. The cycle fold bifurcation (black) is denoted by LPC.

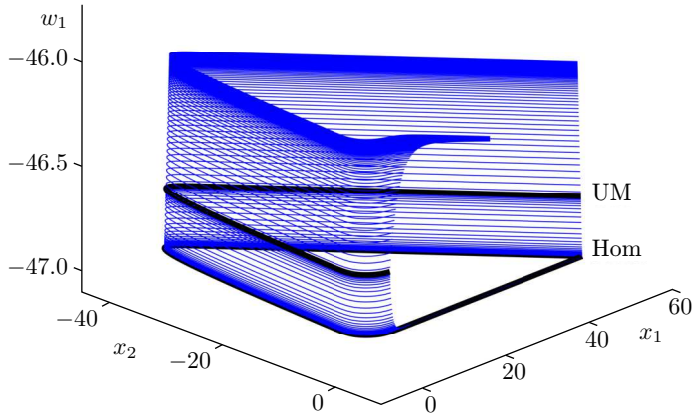


(b) Approximating the unstable manifold (UM) and the saddle homoclinic orbit (Hom).

Figure 2. Detecting global bifurcations in system (2.1)–(2.2) with fixed parameters $a = 4$, $b = 1$, $n = 10$, and $w = 900$.

LPC point in the parameter plane $(w, w_1)$ to form the cycle fold bifurcation curve. This is shown in Figures 3 and 4 with a magenta line. It can be seen that the cycle fold bifurcation curve ends at the saddle homoclinic bifurcation curve (green). This phenomenon was observed in several examples, see, e.g., [8] (Figure 7) and in [14] (Example 8.3 in Section 8.4).

The other global bifurcation that we study is the homoclinic bifurcation. In the two-dimensional case, a homoclinic orbit is the common part of the stable and un-

stable manifold of an equilibrium point. If this point is a saddle, then the homoclinic orbit is called a saddle homoclinic orbit. It may happen that the equilibrium is a saddle-node, then the homoclinic orbit is called a *saddle-node homoclinic orbit*. We can observe both cases in system (2.1)–(2.2). During a homoclinic bifurcation a periodic orbit touches the equilibrium and becomes homoclinic, then it disappears. If the system has a Bogdanov-Takens bifurcation point, then a saddle homoclinic bifurcation curve always starts at this point [14]. To detect the homoclinic bifurcations we can use two different continuation algorithms. One is to start from a limit cycle with large period and continue it by changing a system parameter until its period reaches a prescribed large value, when it is considered to be a homoclinic orbit. The other one, called homotopy method in MatCont [10], is when the unstable manifold of a saddle is approximated first by a solution started near to the saddle. A segment of the unstable manifold is continued until the endpoint reaches the stable eigenspace of the saddle (UM in Figure 2 (b)). Starting from this point the manifold then can be continued to get the endpoint located near the saddle, which indicates an appropriate approximation of the homoclinic orbit (Hom in Figure 2 (b)). We apply the first method to determine the saddle-node homoclinic bifurcation in system (2.1)–(2.2), and the second one for the saddle homoclinic bifurcation which is shown in Figure 2 (b). Once a homoclinic orbit is detected, then it can be continued in the $(w, w_1)$ parameter plane to get the homoclinic bifurcation curves [10], which are shown in Figures 3 and 4. For the fixed parameters $a = 4$, $b = 1$, and $n = 10$, there are two saddle homoclinic bifurcation curves in the system plotted with green. One of them is inside the swallowtail and it starts at the Bogdanov-Takens bifurcation point and ends on the saddle-node curve as it is shown in Figure 4 (b). The other one can be found outside the swallowtail and it also ends on the saddle-node curve, but not at the same point as the previous one. As it can be seen in Figure 3 (b), it has an intersection with the Andronov-Hopf bifurcation curve. The saddle-node homoclinic bifurcation curve (dashed green in Figure 4 (b)) connects the two saddle homoclinic bifurcation curves and lies on the saddle-node curve.

## 4. Phase portraits in the different parameter regions

Now we describe the dynamical behaviour of system (2.1)–(2.2) for parameter pairs $(w, w_1)$ lying in the domains created by the bifurcation curves, namely the saddle-node, Andronov-Hopf, cycle fold and homoclinic bifurcation curves. These bifurcation curves divide the parameter plane into nine domains which are denoted by letters *A*-*I* and are shown in Figures 3 and 4. Now we describe the asymptotic behaviour of system (2.1)–(2.2) for each domain; this is also summarized in Table 1.

| Domain | Equilibrium | Periodic orbit |
|---|---|---|
| $A$ | 1S | - |
| $B$ | 2S, 1U | - |
| $C$ | 2S, 1U | 1U |
| $D$ | 1S, 2U | 1S, 1U |
| $E$ | 1S, 2U | 1S |
| $F$ | 1S, 2U | - |
| $G$ | 3S, 2U | - |
| $H$ | 2S, 3U | 1S |
| $I$ | 2S, 3U | - |

Table 1. Equilibria and periodic orbits in system (2.1)–(2.2). Letters 'S' and 'U' refer to stable and unstable equilibria and periodic orbits. The numbers represent their number in each domain.

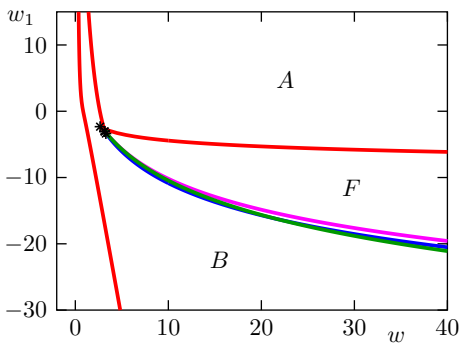


(a) All detected local and global bifurcation curves.

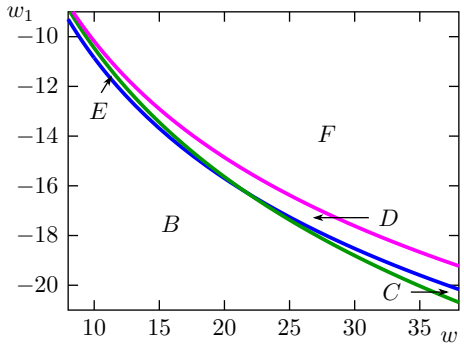


(b) The intersection of the Andronov-Hopf and saddle homoclinic bifurcation curves.

Figure 3. Saddle-node (red), Andronov-Hopf (blue), cycle fold (magenta), saddle homoclinic (green) and saddle-node homoclinic (dashed green) bifurcation curves and their magnifications in system (2.1)–(2.2) with fixed parameters $a = 4$, $b = 1$, and $n = 10$. CP is the cusp point and BT is the Bogdanov-Takens bifurcation point.

The model has a single globally stable steady state if the parameter pair $(w, w_1)$ is in domain $A$. Crossing the saddle-node bifurcation curve towards domain $B$ we can find three equilibria. The first and the third ones are stable, the middle one is a saddle. (The equilibria here and below are ordered according to their first coordinate.) Entering domain $C$, an unstable periodic orbit appears around the first steady state via saddle homoclinic bifurcation. The Andronov-Hopf bifurcation is supercritical, that is, if we step into domain $D$, the first fixed point loses its stability and a stable limit cycle appears around it. The unstable periodic orbit remains around them. Because of the intersection of the saddle homoclinic and Andronov-

Hopf bifurcation curves, only the stable limit cycle exists around the first steady state in domain $E$. The stable and unstable periodic orbits collide and disappear via cycle fold bifurcation, that is, in domain $F$ only the three equilibria can be found without any periodic orbit. The system has five steady states inside the swallowtail. The first and fifth of them are always stable and the second and the fourth are saddles. In domain $G$ the third equilibrium is stable but it becomes unstable as Andronov-Hopf bifurcation occurs and a stable periodic orbit appears around it in domain $H$. This limit cycle becomes homoclinic and it disappears via saddle homoclinic bifurcation, so only the five equilibria remain in the phase portrait belonging to domain $I$.

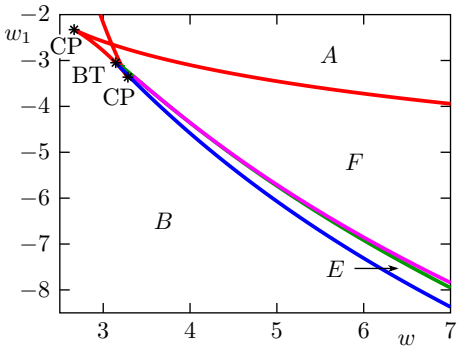


(a) Magnification of the swallowtail. The cycle fold bifurcation curve ends at the saddle homoclinic bifurcation.

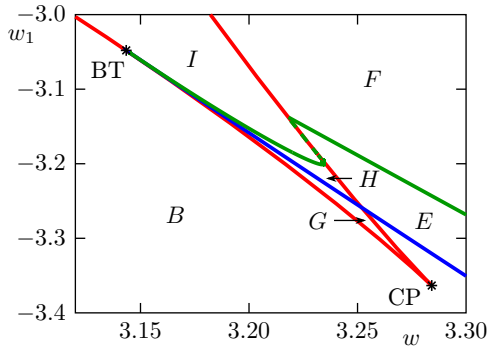


(b) The right-hand side of the swallowtail. The saddle-node homoclinic bifurcation curve connects the two saddle homoclinic bifurcation curves.

Figure 4. Saddle-node (red), Andronov-Hopf (blue), cycle fold (magenta), saddle homoclinic (green) and saddle-node homoclinic (dashed green) bifurcation curves and their magnifications in system (2.1)–(2.2) with fixed parameters $a = 4$, $b = 1$, and $n = 10$. CP is the cusp point and BT is the Bogdanov-Takens bifurcation point.

Now we show how the phase portraits of system (2.1)–(2.2) change via three important bifurcations. First, we fix $w$ and vary the value of $w_1$ to cross the homoclinic (green) and Andronov-Hopf bifurcation (blue) curves. If the parameter pair is in domain $B$, then there is no periodic orbit. Figure 5 (a) shows the phase portrait when the parameter pair is on the homoclinic bifurcation curve, i.e., on the boundary of domains $B$ and $C$. We have then a saddle homoclinic orbit where the unstable periodic orbit, which remains to exist in domains $C$ and $D$, is born. Crossing the Andronov-Hopf bifurcation curve, i.e., entering domain $D$, a stable periodic orbit appears. In Figure 5 (b), the coexisting stable and unstable limit cycles can be seen surrounding the unstable steady state.

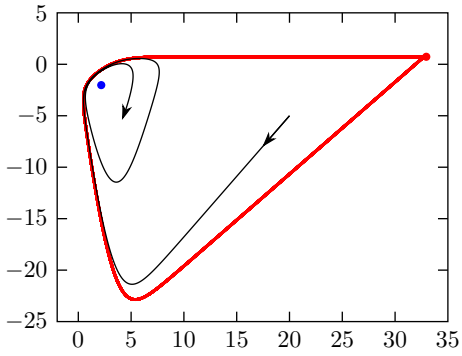


(a) Saddle homoclinic orbit surrounding the stable equilibrium. The parameter pair $(w, w_1)$ lies on the boundary of domains $B$ and $C$ at $w_1 = -28.55$.

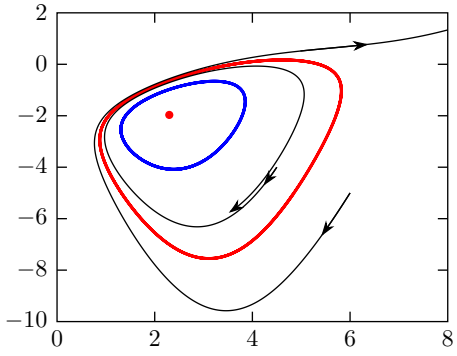


(b) Unstable steady state and the stable and unstable periodic orbits around it. The parameter pair $(w, w_1)$ is in domain $D$ with $w_1 = -26$.

Figure 5. Phase portraits in system (2.1)–(2.2) with fixed parameters $a = 4$, $b = 1$, $n = 10$, and $w = 100$.

Second, we fix $w$ and vary the value of $w_1$ to cross the homoclinic (green) curve inside the swallowtail. The stable limit cycle existing for parameter pairs in domain $H$ is shown in Figure 6 (b). This limit cycle becomes a saddle homoclinic orbit shown in Figure 6 (a) when the parameter pair is on the boundary of domains $H$ and $I$. The limit cycle disappears via saddle homoclinic bifurcation as the parameter pair enters domain $I$.

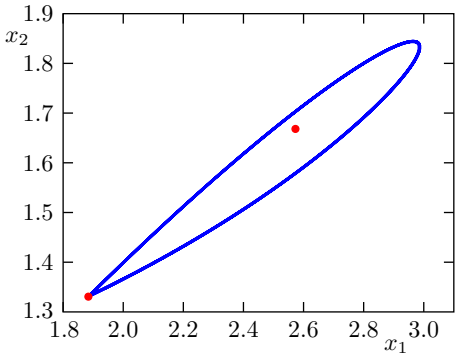


(a) Saddle homoclinic orbit surrounding the unstable equilibrium. The parameter pair $(w, w_1)$ lies on the boundary of domains $H$ and $I$.

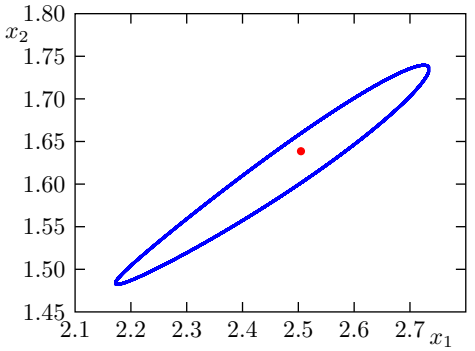


(b) Unstable steady state and the stable periodic orbit around it. The parameter pair $(w, w_1)$ is in domain $H$.

Figure 6. Phase portraits of system (2.1)–(2.2) for parameter pairs inside the swallowtail and with fixed parameter values $a = 4$, $b = 1$, $n = 10$, and $w = 3.23$.

Finally, we fix $w$ and let $w_1$ vary in such a way that the parameter pair $(w, w_1)$ moves from domain $I$ to domain $E$ by crossing the saddle-node homoclinic bifurcation curve and then moving forward to cross the saddle homoclinic curve and entering domain $F$. The phase portraits belonging to parameter pairs lying (a) on the boundary of $I$ and $E$, (b) in the domain $E$ and (c) on the boundary of $E$ and $F$ are shown in Figure 7. We can see that a stable limit cycle appears via saddle-node homoclinic bifurcation on the boundary of $I$ and $E$, then it becomes a saddle homoclinic orbit on the boundary of $E$ and $F$ and then disappears in $F$.

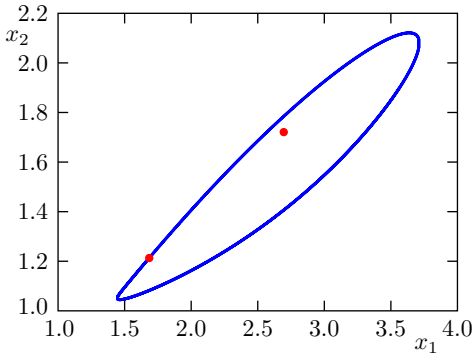


(a) Saddle-node homoclinic orbit for a parameter pair $(w, w_1)$ lying on the boundary of domains $I$ and $E$ at $w_1 = -3.16335$.

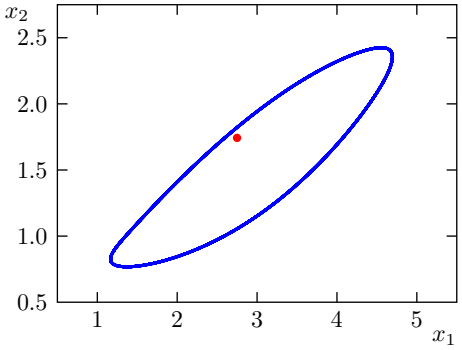


(b) Unstable steady state and the stable periodic orbit around it for a parameter pair $(w, w_1)$ in domain $E$ at $w_1 = -3.15$.

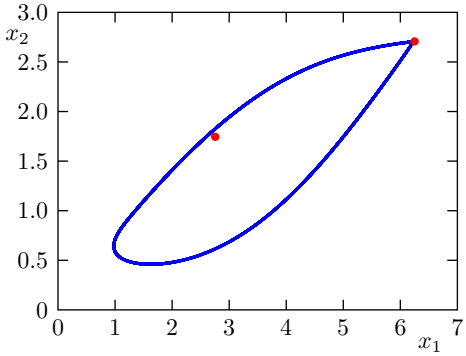


(c) Saddle homoclinic orbit for a parameter pair $(w, w_1)$ lying on the boundary of domains $E$ and $F$ at $w_1 = -3.1486344$.

Figure 7. Birth of a stable periodic orbit via saddle-node homoclinic bifurcation and its disappearance via saddle homoclinic bifurcation with fixed parameters $a = 4$, $b = 1$, $n = 10$, and $w = 3.225$. An unstable steady state is surrounded by the homoclinic and periodic orbits.

## 5. Conclusion

In this paper our main goal was to classify some possible long-time dynamical behaviours of the Hopfield model given in (1.1) when the weight matrix has a special non-symmetric structure. The starting point is a fully connected network when all non-diagonal weights are equal and positive, i.e., all neurons are identical and excitatory. This simple special case can be completely characterized, since all trajectories tend to steady states. The effect of an inhibitory neuron is in the focus of this paper. We considered the case when there are $n-1$ identical neurons with the same positive weight $w$ and only one neuron with an arbitrary weight $w_1$. We assumed that the neurons do not receive any external input and they do not connect to themselves directly.

The local bifurcations can be characterized and determined analytically. It turned out that saddle-node and Andronov-Hopf bifurcations may occur leading to bistability or a periodic orbit. We also investigated the numerical detection of global bifurcations to describe the dynamics of the model in the whole parameter region. Saddle-homoclinic, cycle fold and saddle-node homoclinic codimension 1 bifurcation curves were detected using MatCont numerical toolbox of MATLAB. We studied the behaviour of the model in each domain created by the bifurcation curves. We showed that there can be one, three or five steady states and a stable and an unstable periodic orbit may exist together yielding a rich dynamical behaviour.

These results show that even a single inhibitory neuron can create several new dynamical phenomena. Hence, it may be interesting to study the behaviour of the system with more complex weight matrices. This could be the subject of future research.

*References*


[1] *R. D. Beer*: On the dynamics of small continuous-time recurrent neural networks. Adapt. Behav. *3* (1995), 469–509. doi

[2] *R. D. Beer*: Parameter space structure of continuous-time recurrent neural networks. Neural Comput. *18* (2006), 3009–3051. zbl MR doi

[3] *M. Breakspear*: Dynamic models of large-scale brain activity. Nature Neurosci. *20* (2017), 340–352. doi

[4] *N. Brunel*: Dynamics of sparsely connected networks of excitatory and inhibitory spiking neurons. J. Comput. Neurosci. *8* (2000), 183–208. zbl doi

[5] *A. Ecker, B. Bagi, E. Vértes, O. Steinbach-Németh, M. R. Karlócai, O. I. Papp, I. Miklós, N. Hájos, T. F. Freund, A. I. Gulyás, S. Káli*: Hippocampal sharp wave-ripples and the associated sequence replay emerge from structured synaptic interactions in a network model of area CA3. eLife *11* (2022), Article ID e71850, 29 pages. doi

[6] *B. Ermentrout*: Neural networks as spatio-temporal pattern-forming systems. Rep. Progr. Phys. *61* (1998), Article ID 353, 78 pages. doi

[7] *B. Ermentrout, D. H. Terman*: Mathematical Foundations of Neuroscience. Interdisciplinary Applied Mathematics 35. Springer, New York, 2010. zbl MR doi

[8] *D. Fasoli, A. Cattani, S. Panzeri*: The complexity of dynamics in small neural circuits. PLoS Comput. Biology *12* (2016), Article ID e1004992, 35 pages. doi

[9] *D. Fasoli, A. Cattani, S. Panzeri*: Bifurcation analysis of a sparse neural network with cubic topology. Mathematical and Theoretical Neuroscience. Springer INdAM Series 24. Springer, Cham, 2017, pp. 87–98. zbl MR doi
[10] *W. Govaerts, Y. A. Kuznetsov, V. DeWitte, A. Dhooge, H. G. E. Meijer, W. Mestrom, A. M. Rietand, B. Sautois*: MATCONT and CL_MATCONT: Continuation Toolboxes in Matlab. Gent University and Utrecht University, Gent and Utrecht, 2011.
[11] *S. Grossberg*: Nonlinear neural networks: Principles, mechanisms, and architectures. Neural Netw. *1* (1988), 17–61. doi
[12] *J. J. Hopfield*: Neural networks and physical systems with emergent collective computational abilities. Proc. Natl. Acad. Sci. USA *79* (1982), 2554–2558. zbl MR doi
[13] *J. J. Hopfield*: Neurons with graded response have collective computational properties like those of two-state neurons. Proc. Natl. Acad. Sci. USA *81* (1984), 3088–3092. zbl doi
[14] *Y. A. Kuznetsov*: Elements of Applied Bifurcation Theory. Applied Mathematical Sciences 112. Springer, New York, 2004. zbl MR doi
[15] *L. Perko*: Differential Equations and Dynamical Systems. Texts in Applied Mathematics 7. Springer, New York, 2001. zbl MR doi
[16] *T. Trappenberg*: Fundamentals of Computational Neuroscience. Oxford University Press, Oxford, 2010. zbl MR
[17] *A. Windisch, P. L. Simon*: The dynamics of the Hopfield model for homogeneous weight matrix. Ann. Univ. Sci. Budap. Rolando Eötvös, Sect. Math. *64* (2021), 235–247. zbl

*Authors' addresses*: *Anita Windisch*, Department of Applied Analysis and Computational Mathematics, Institute of Mathematics, Eötvös Loránd University, Pázmány Péter sétány 1/C, 1117 Budapest, Hungary, e-mail: `anita.windisch@ttk.elte.hu`; *Péter L. Simon* (corresponding author), Department of Applied Analysis and Computational Mathematics, Institute of Mathematics, Eötvös Loránd University, Pázmány Péter sétány 1/C, 1117 Budapest, Hungary; Numerical Analysis and Large Networks Research Group, Hungarian Academy of Sciences, Széchenyi István sqr. 9, 1051 Budapest, Hungary, e-mail: `peter.simon@ttk.elte.hu`.